M1002

Simulation of *in vitro* Caco-2 Papp from Molecular Structure Estimation of Intracellular K_m for Efflux Transporters

Michael B. Bolger, Viera Lukacova, James M. Mullin, Ke Szeto

Simulations Plus, Inc., 42505 10th Street West, Lancaster, CA 93534, USA

Abstract

Purpose

To build *in silico* models based on molecular structure that estimate the rate of passive diffusion into and out of the cell membrane and to combine those estimates with a cellular simulation of Caco-2 apparent permeability to determine the intracellular unbound K_m for efflux transporters.

Methods

A cellular simulation program (MembranePlus™, Simulations Plus, Inc. Lancaster CA) of Caco-2 apparent permeability was used to calibrate a simple QSAR model of the passive rate into and out of the cellular membrane bilayer for 22 diverse compounds. This was compared to the drug partitioning of forward and reverse rate constant method of Kubinyi (Kubinyi 1978). A separate cellular simulation for 8 different concentrations of digoxin with and without inhibition of P-glycoprotein (P-gp) (Troutman and Thakker 2003) was used to fit the value of the intracellular unbound K_m for P-gp. Finally, the K_m value for P-gp determined from fitting in the cellular simulation was used to build a mechanistic oral absorption and physiologically based pharmacokinetic (PBPK) model of digoxin using GastroPlus™ (Simulations Plus, Inc., Lancaster, CA). To account for the *in vivo* distribution and clearance of digoxin, the PBPK model incorporated permeability-limited liver, kidney, and muscle tissues with basolateral influx and apical efflux transporters. The PBPK model simulation results were compared to literature plasma concentration-time (Cp-time) data for escalating doses of digoxin by intravenous and oral administration routes (Ochs, et al. 1978; Greiner, et al. 1999).

Results

The cellular simulation for 22 diverse drug molecules using the QSAR model was more accurate than a model based on Kubinyi's drug partitioning theory. The fitted intracellular unbound K_m value for digoxin (95.3 μM) was significantly lower than K_m values measured *in vitro* by Troutman et al. in either the absorptive (1150 μM) or secretory (177 μM) directions (Troutman and Thakker 2003). The PBPK simulations of Cp-time compared well to the observed clinical data for digoxin.

Conclusions

A combination of cellular simulation of *in vitro* experiments and PBPK modeling of *in vivo* Cp-time profiles can provide a good estimation of the significance of efflux transporters on dose linearity of absorption, distribution, and excretion.

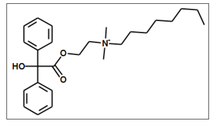

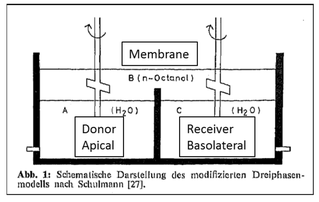

Abb. 1: Schematische Darstellung des modifizierten Dreiphasenmodells nach Schuhmann [27].

Figure 1: Octanol/water partitioning kinetics experiment for calibration of logP (Lippold, 1975)

References

Greiner, B., et al. (1999). J Clin Invest 104(2): 147-53.
Kubinyi, H. (1978). J Pharm Sci 67(2): 262-3.
Lippold VBC, Arzneimittel-Forschung, 25(6):843 (1975)
Ochs, H. R., et al. (1978). Am Heart J 96(4): 507-11.
Jounela, A.J., et al. (1975). Eur. J. Clin. Pharmacol. 8:365-370.
Troutman, M. D. and D. R. Thakker (2003). Pharm Res 20(8): 1200-9.

Results: MembranePlus

MembranePlus Simulation of octanol/water partitioning:

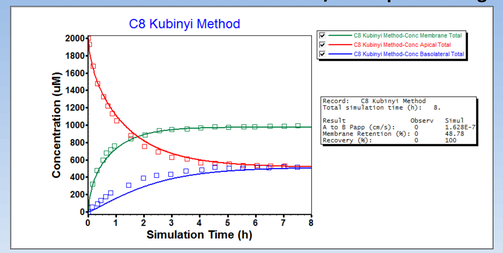

Figure 2: MembranePlus simulation of N-2-benzoyloxyethyl-N,N-dimethyl-(2-hydroxyethyl)-N-octyl-ammonium bromide from donor (water) into octanol and back into receiver (water) compartments. Symbols are experimental concentrations and lines are simulated by MembranePlus. Rate constant for entry into octanol (k_i = 0.864 h^{-1} and exit from octanol (k_o = 0.477 h^{-1}). Partition coefficient was (P = k_i/k_o = 1.82. logP = 0.26).

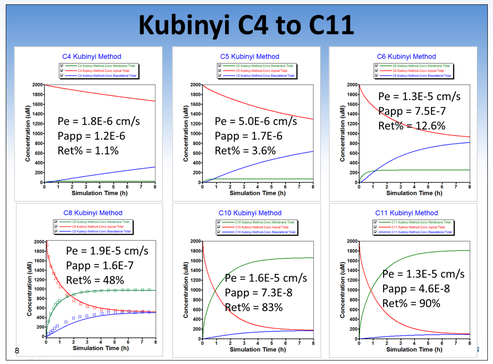

Figure 3: MembranePlus simulation of N-2-benzoyloxyethyl-N,N-dimethyl-(2-hydroxyethyl)-N-(C4 – C11)-alkyl-ammonium bromides.

Results: MembranePlus

The MembranePlus structure-based model was trained on Caco-2 data from 44 experiments*. Molecular descriptors used in the multiple linear regression model included: logP, presence of non-benzene ring structures, and hydrogen bonding features.

* 22 drugs A->B Papp at pH 7.4 and pH 6.5
Data courtesy of Absorption Systems, LP

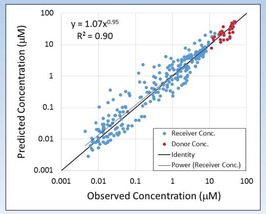

A

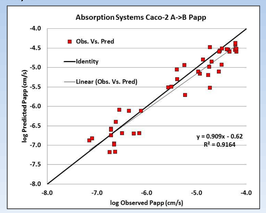

B

Figure 4A: Observed vs. predicted apical and basolateral concentrations of the 44 Caco-2 experimental dataset using the default Structure-Based Membrane Transport model

Figure 4B: Observed vs. predicted Caco-2 Papp of the 22-compound Caco-2 dataset using the default Structure-Based Membrane Transport model

Digoxin physicochemical properties:
logP = 1.38, Aq. Sol. = 47 μg/mL
Caco-2 Papp (cm/s) A->B = 0.0076 x 10^{-5} B->A = 0.76 x 10^{-5}
First step is to calibrate the structure-based membrane transport model coefficient for H-bonding to oxygens to match P-gp inhibited Papp.

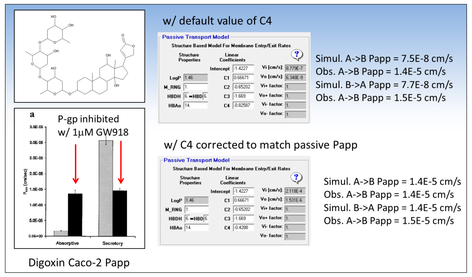

Results: MembranePlus

The Caco-2 *in vitro* K_m for P-gp was determined to be 240 μM (Troutman, 2003). However, the intracellular unbound P-gp K_m for digoxin was found to be 95.3 μM by fitting B->A Papp with MembranePlus across experiments run at eight different concentrations and validated in a separate experiment using kinetic data at five concentrations (Figure 5).

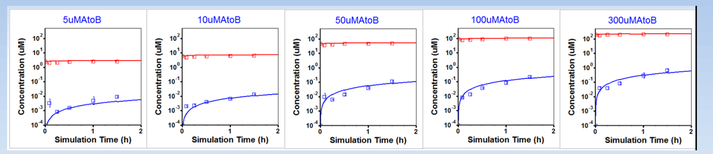

Figure 5: Observed (symbols) and predicted (lines) apical and basolateral concentrations of digoxin using the fitted intracellular unbound K_m value of 95.3 μM.

Results: GastroPlus

The GastroPlus PBPK model for digoxin included: passive absorption and P-gp efflux in the gut, a permeability-limited liver with passive and Sodium-dependent MultiVitamin (SMVT) transporter-mediated basolateral influx, MRP3-mediated basolateral efflux, and P-gp-mediated apical efflux. Permeability-limited kidney with passive and OATP4C1-mediated basolateral influx and active apical efflux, as well as permeability-limited muscle tissue with digoxin binding to Na^+K^+ATPase were employed. Figure 6 shows results for intravenous and PO formulations of digoxin.

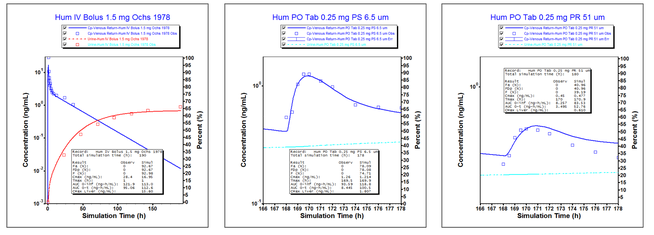

A B C

Figure 6A: Observed (symbols) vs. predicted plasma conc. (blue) and urinary excretion (red) of digoxin assuming the intracellular unbound P-gp K_m value of 95.3 μM (Ochs, 1978).
Figure 6B: Observed (symbols) vs. predicted plasma conc. (blue) of digoxin for a PO formulation with 6.5 μm radius particle size (Jounela, 1975).
Figure 6C: Observed (symbols) vs. predicted plasma conc. (blue) of digoxin for a PO formulation with 51 μm radius particle size (Jounela, 1975).

MembranePlus Mechanistic Cellular Simulation Model

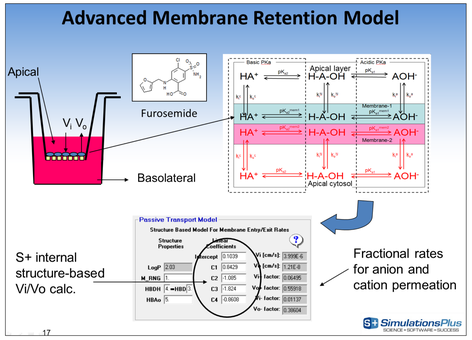

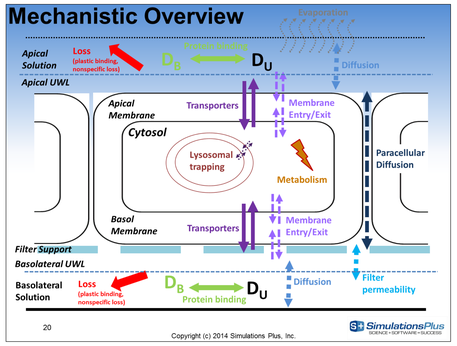

CONCLUSIONS

The classical Kubinyi method and structure-based estimation of membrane kinetic parameters both work well for simulation of *in vitro* organic solvent partitioning; however, the MembranePlus structure-based estimation of rate into and out of biological membranes better explains the cellular permeability of diverse chemicals.

Caco-2 cellular simulations can be used to estimate the intracellular unbound K_m for substrates of efflux transporters. Use of those K_m values in mechanistic absorption and PBPK simulations helps to explain the ADME of complex molecules like digoxin.

SimulationsPlus
SCIENCE + SOFTWARE = SUCCESS